Organic & Biomolecular Chemistry

Accepted Manuscript

This article can be cited before page numbers have been issued, to do this please use: K. Ben Haj Salah, S. Das, N. Ruiz, V. Andreu, J. Martinez, E. Wenger, M. Amblard, C. Didierjean, B. Legrand and N. Inguimbert, *Org. Biomol. Chem.*, 2018, DOI: 10.1039/C8OB00686E.

ROYAL SOCIETY OF CHEMISTRY

rsc.li/obc

View Article Online
DOI: 10.1039/C8OB00686E

Organic and Biomolecular Chemistry

ARTICLE

How are 1,2,3-Triazoles accommodated in helical secondary structures?

Received 00th January 20xx,
Accepted 00th January 20xx

DOI: 10.1039/x0xx00000x

www.rsc.org/

Khoubaib Ben Haj Salah,[a] Sanjit Das,[a] Nicolas Ruiz,[b] Vanessa Andreu,[c] Jean Martinez,[d] Emmanuel Wenger,[e] Muriel Amblard,[d] Claude Didierjean,[e] Baptiste Legrand,*[d] and Nicolas inguimbert *[c]

1,4-disubstituted-1,2,3-triazole (Tz) is widely used in peptides as a trans-amide bond mimic, despite having hazardous effects on the native peptide activity. The impact of amide bond substitution by Tz in peptide secondary structures is scarcely documented. We performed a Tz scan, by systematically replacing peptide bonds following the Aib residues by Tz on two model peptaibols: alamethicin F50/5 and bergofungin D, which adopt stable α- and 3_{10} helices, respectively. We observed that the Tz insertion, independently of its position in the peptide sequences, abolished their antimicrobial activity. The structural consequences of this insertion were further investigated using CD, NMR and X-ray diffraction. Importantly, five crystal structures that incorporated Tz were solved, showing various degrees of alteration of the helical structures, from minor structural perturbation of the helix to partial disorder. Together, these results showed that Tz insertions impair helical secondary structures.

Introduction

Since the pioneering work of Meldal and Sharpless, copper (I)-catalyzed azide-alkyne cycloaddition (CuAAC) affording 1,4-disubstituted-1,2,3-triazoles (Tz) have generated broad interest throughout the field of chemistry.[1,2,3] Peptide chemistry is certainly one of the fields that has benefited most from click chemistry.[4,5,6,7] CuAAC was applied to the synthesis of otherwise inaccessible cyclic peptidomimetics,[8] to the ligation of unprotected peptide fragments to yield Tz-containing proteins.[9,10] The incorporation of Tz into peptides and proteins stabilizes discrete conformations such as β-strand,[11] and α-helix through side chain to side chain cyclization.[12,13,14] In several studies, the Tz ring was considered as a non-classical amide bond bioisostere that could accommodate any peptide secondary structure.[15,16,17] Its hydrogen bonding capacity and its planar character have raised considerable interest for the use of the 1,4-disubstituted Tz as a *trans* peptide bond surrogate (Figure 1). Consequently, the concept of Tz as an amide bond mimic has emerged and was extensively applied on cyclic peptides.[18,19,20] The insertion of Tz within the backbones of linear biologically active peptides such as bombesin[21,22] or kisspeptin[23] increased activity by extending metabolic stability, whereas the activity of enkephalin decreased.[24] However, the impact of the Tz incorporation on the three-dimensional structure of these peptides has not been studied despite the close relationship between their conformation and activity.[25,26] To the best of our knowledge, only two studies have monitored Tz insertion within the sequence of alpha-helical peptides. In the first study, the pLI mutant of the 33 amino acid long α-helical coiled coil GCN4 transcription factor was selected as a model.[27] A comparison of the X-ray structure of the native peptide with three analogues where the X-Leu (X: Lys or Glu) dipeptides were replaced by Gly[ψTz]Leu **3a** showed different outcomes ranging from partially disordered to fully conserved structures. As the native sequence was not entirely conserved, to distinguish the effect of Tz incorporation from that of the substitution of the Lys or Glu residues by the flexible Gly residue was not an insignificant task. In a recent study, a structured helical α-aminoisobutyric acid (Aib) oligomer with the sequence Cbz-Phe-$(Aib)_4$-Aib^6-$(Aib)_4$-Gly-NH_2 was fully destabilized in solution by replacing Aib^6-Aib^7 dipeptide with Gly[ψTz]Aib.[28] Different results were reported in response to differences in peptide sequence, position and the number of Tz substitutions. However, no clear trend emerged, prompting researchers to anticipate Tz conformational effects through molecular modelling.[29] The specific properties of Tz compared with the amide bond (stretching of the Cα–Cα distance of ~1 Å, higher dipole moment and two nitrogen atoms as hydrogen bond acceptors, Figure 1), do not appear to be fully compatible with peptide helical structures. In this study we investigated

[a] USR 3278 CRIOBE, PSL Research University, EPHE-UPVD-CNRS, Université de Perpignan Via Domitia, Laboratoire d'Excellence « CORAIL ». Bâtiment T, 58 avenue P. Alduy, 66860 Perpignan, France. E-mail: nicolas.inguimbert@univ-perp.fr
[b] Laboratoire Mer Molécules Santé. Université de Nantes, UFR de Sciences pharmaceutiques et biologiques, 9 rue Bias - BP 61112, 44035 Nantes, France.
[c] Akinao, 58 avenue P. Alduy, 66860 Perpignan, France.
[d] Institut des Biomolécules Max Mousseron (IBMM), Univ Montpellier, CNRS, UM, ENSCM, Montpellier, France. E-mail: baptiste.legrand@umontpellier.fr
[e] CRM2, UMR UL-CNRS 7036, Faculté des Sciences et Technologies, Université de Lorraine, 70239 Boulevard des Aiguillettes, 54506 Vandoeuvre-lès-Nancy, France.
Electronic Supplementary Information (ESI) available: [details of any supplementary information available should be included here]. See DOI: 10.1039/x0xx00000x

the effects of Tz substitution on the activity and structures of two stable helical peptaibols: the 20-mer alamethicin F50/5 (Alm) **4a** and the 14 amino acid residues of bergofungin D (BergD) **5a**.[30,31] These antibacterial peptides contain high proportions of Aib (25-50%)[32,33] That promote α- and 3_{10}-helices, and that are stabilized by (*i*,*i*+4) and (*i*,*i*+3) C=O⋯H-N hydrogen bonding patterns, respectively.[30,34] The Alm structure is broken by a proline in position 14 delineating two helices (Figure 3). It can multimerize to form voltage-gated channels enabling its biological effect.[35,36]

Results and Discussion

Synthesis and biological activity of Alm and BergD analogues.

We previously showed that Fmoc protected Tz-containing dipeptides **3b** (Figure 1) are attractive precursors because they are easily obtained in a few steps and are fully compatible with solid-phase peptide synthesis (SPPS).[37,38] The Aib-Xaa dipeptides, evenly distributed in both peptaibol sequences, allowed for a Tz scan using Aib[ψTz]Xaa surrogates all along the Alm and BergD sequences (Table 1). We have synthesized nine and five analogues of Alm and BergD, respectively, containing single or multiple Tz substitutions. The analogues containing multiple Tz insertions results from the combination of all single substitutions in one peptide. As Alm and Berg D contained a AibAibXaa sequence two substitution possibilities existed: Aib[ψTz]Aib or Aib[ψTz]Xaa thus leading for each peptide to two possibilities **4i-j** for Alm and **5e-f** for BergD. These peptides were assembled on 2-chlorotrityl resin preloaded with phenylalaninol according to the general Fmoc/tBu microwave-assisted SPPS procedure. Stepwise synthesis of the peptaibols analogues **4-5** at a 0.1 mmol scale using single coupling steps for amino acids or for dipeptides **3b** proceeded smoothly, and the final products were obtained with correct yields after purification (Table 1).[39,40] Compound structures and purity were ascertained by LC-MS, ^{1}H, ^{13}C and ^{15}N NMR (Supporting information S3-S18 and S30-56).

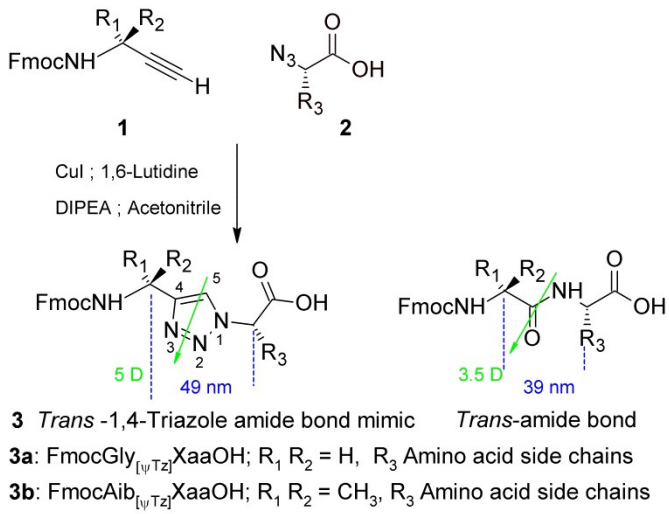

Figure 1. Synthesis of Fmoc-1,4-disubstituted 1,2,3-triazolodipeptides **3** and comparison of trans-amide bond with 1,4-disubstituted 1,2,3-triazole **3**. Distance between Cα-Cα, value of the dipole moment and triazole numbering are given.

Table 1. Yields and CD spectroscopy data for peptaibols **4** and **5**

Cpd	Tz position	Yield[a]	λ_{min} (nm)	$[\theta]_{202-208}$ (deg cm² dmol^{-1})	$[\theta]_{220-231}$ (deg cm² dmol^{-1})	R= $[\theta]_{222}/[\theta]_{208}$	HC[b]
Alamethicin sequence **4a**: AcUP^{2}UA^{4}UA^{6}QU^{8}VU^{10}GL^{12}UP^{14}VU^{16}UQ^{18}QFol [c]							
4a		45	208-221	-14971	-12018	0.8	31
4b	3-4	28	208-220	-12566	-8558	0.7	22
4c	5-6	34	207-225	-4595	-2957	0.6	>1
4d	8-9	20	207-224	-7592	-5182	0.7	13
4e	10-11	42	207-224	-10033	-7411	0.7	19
4f	16-17	45	208-220	-11798	-8369	0.7	22
4g	17-18	28	208-223	-15976	-12094	0.7	31
4h	13-14[d]	48	208-225	-13571	-11108	0.8	28
4i	multiple[e]	37	201-231	-2542	-6225	-	*nh*
4j	multiple[f]	38	201-231	-3753	-2487	-	*nh*
Bergofungin D sequence **5a**: AcVU^{2}UV^{4}GL^{6}UU^{8}OQ^{10}UO^{12}UFol [c]							
5a		63	208-222	-7065	-3338	0.5	9
5b	2-3	56	207-234	-435.7	-1018	-	*nh*
5c	3-4	34	208-234	2210	-668	-	*nh*
5d	7-8	55	204-234	-2565	-2224	-	*nh*
5e	2-3, 7-8	54	203-237	-656	-887	-	*nh*
5f	3-4, 7-8	54	202-234	1423	-2286	-	*nh*

[a] % after HPLC purification ; [b] Helical content; nh: non characteristic helix signature; [c] Ac: acetyl; Fol: Phenylalaninol; U: Aib; O: Hydroxyproline. [d] Pro14 was additionally mutated by an Aib residue in the peptide 4h. [e] in positions 3-4, 5-6, 8-9, 10-11, 16-17 and [f] 3-4, 5-6, 8-9, 10-11, 17-18.

First, biological activity of the Alm analogues was evaluated at a concentration of 50 µg/mL, a level ten-fold higher than the MIC determined for Alm **4a**. Interestingly, in contrast to the native Alm, all analogues were found inactive in a growth inhibition assay on gram positive bacteria (*Bacillus subtilis*), a primary target of peptaibols. On human KB cell lines, only compounds **4b** (IC_{50}: 189 ± 24 µg/ml) and **4f** (IC_{50}: 85 ± 18 µg/mL) are somewhat cytotoxic. BergD and its analogues were all inactive as it was recently observed for the closely related bergofungin A (BergA).[34] Thus, we showed that Tz insertion abolished the antimicrobial activity of Alm regardless of the position of the mutation and remained slightly cytotoxic for **4b** and **4f**.

Structure of Alm and BergD analogues.

Far-UV CD spectroscopy allowed for the helical propensity of the various analogues in solution to be assessed (Figure 2). As expected, the CD spectra of the native Alm **4a** and BergD **5a** displayed the characteristic profile of a helix with a positive maximum around 195 nm and two negative maxima around 209 and 228 nm. The helical content (HC) was 31% for Alm and 9% for BergD.[41] Even if controversial,[42,43,44] the $[\theta]_{222}/[\theta]_{208}$ ellipticity ratio was 0.80 for Alm and 0.47 for BergD indicating a predominant α-helix for Alm and most likely a 3_{10} type helix for BergD.

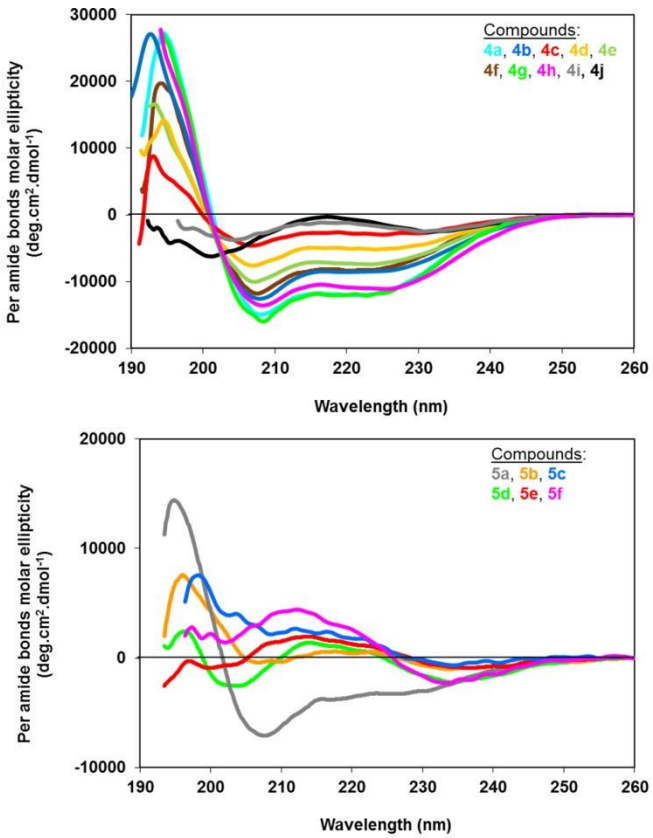

Figure 2: CD spectra of Alm F50/5, BergD and analogues **4b-j** and **5b-f** in methanol at 20°C.

These results were fully consistent with those previously obtained for the Alm while BergD probably adopted a 3_{10} helix structure similar to that of BergA.[30,34] The maxima of the signal intensities for the analogues generally decreased and in some cases, the CD spectra did not display a helix profile. First, we observed that the CD spectra were similar for Alm **4a** and the analogue **4g** when the Tz was incorporated at the C-terminal extremity in position (17-18). A decrease of the signal by one third (HC decreased from 31% to ~20%) was observed when the Tz insertion was localized at the N- or C-terminal part of the peptide **4b** (3-4), and **4f** (16-17), respectively or at the center of the sequence **4e** (10-11), near the Alm hinge. When the Tz was introduced in the middle of the N-terminal helix, the helicity dropped to around 13% for **4d** (8-9), and was totally lost in the case of **4c** (5-6). Importantly, a single Tz substitution regardless of its position in the BergD analogues **5b-d** strongly affected the 3_{10}-helix CD signature (Figure 2). Also, multiple Tz insertions in both peptaibol analogues **4i**, **4j**, **5e** and **5f** shared weak CD signals with negative maxima shifted around 200 nm and 230 nm, and the positive maxima around 195 nm could no longer be observed. Thus, a single Tz mutation in the BergD as well as multiple Tz insertions in both peptaibol sequences may prevent the helix formation. In addition, it has been shown that the Pro14Ala or Pro14Aib mutations restored the continuity of the hydrogen bond network and stabilized the Alm helix structure.[45,46] Here, we replaced the Aib^{13}Pro^{14} dipeptide with Aib^{13}[ψTz]Aib^{14} to yield **4h**. Very close CD profiles were recorded for **4a** and **4h** indicating that their helix structures exhibited similar stability. We further investigated the structural impact of such Tz insertions using high-resolution techniques such as X-ray crystallography and NMR spectroscopy.

To our knowledge, only the work of Ghadiri et al.[27] reported crystal structures of helical peptides containing Tz in their backbones (with resolutions around 2.2 Å). Fortunately, we obtained single crystals suitable for X-ray diffraction studies of Alm analogues **4g**, **4h**, and, of BergD **5a** and analogues **5b**, **5d** and **5f** at near atomic resolution. Except for compound **5f**, all of the analogues adopted fully helical structures with the N^2 and C^5-H components of the Tz involved in hydrogen bonds. These data showed that estimates of helicities with CD spectroscopy were largely underestimated due to the presence of numerous achiral Aib residues as previously reported.[47,48] We first compared the crystal structure of the Alm (PDB entry 1amt) with those of **4g** and **4h** which were the analogues that retained helical contents similar to those of the native Alm (~30%) (Figure 3). The N-terminal sequences (from residue 1 to 16) of both compounds **4g** and Alm were closely related with a root mean square deviation (rmsd) of 0.32 Å on Cα atoms (Figure S2-1). In **4g**, the sequence following the Tz insertion (17-18) was presumed to be unfolded because no electron density was observed for this region in the Fourier-difference map. In contrast, **4h** was completely folded but the Tz incorporation in position 13-14 associated with the substitution of Pro^{14} by Aib induced a large 30° bend of the C-terminal moiety in the opposite direction from that of the native structure, although the first twelve residues were superimposable (rmsd of 0.27 Å on Cα atoms) (Figures 3A and S2-1). In Alm and **4g**, the hydrogen bond network was disrupted by Pro^{14}, making Aib^{10} and Gly^{11} carbonyl oxygen atoms solvent-accessible. In **4h**, the Pro^{14}Aib substitution plus the Tz insertion allowed for the formation of a complete network of interactions, including a weak Tz-C^5-H….O=C-Aib^{10} (d_{C5H-O} = 2.74 Å), a strong Val^{15}-NH…O=C-Gly^{11} (d_{NH-O} = 2.28 Å) and Aib^{17}-N-H….N^2-Tz, (d_{NH-N2} = 2.51 Å) hydrogen bonds, which affected the native Alm helix shape and altered the distribution of the polar groups on its surface, thereby masking the Aib^{10} and Gly^{11} carbonyl oxygens from the solvent (Figure 2A and table S2-3).[30] We observed notable differences in the torsion angle values of Leu^{12} and the ψ angles of Pro^{14} and Aib^{14} in **4a** (ψ = -28°) and **4h** (ψ = -64°), respectively (Table S2-2). The partial unfolding of **4g** and the structural alteration of **4h**, both of which affected the C-terminal part of the peptide, could explain the loss of biological activity of analogues **4g** and **4h**. These results highlighted the role played by the Gly^{11}(Xaa)$_3$Pro^{14} hinge and the less organized C-terminal part of Alm in the bundle formation required for biological activity.[45,49] Moreover, **4g** and **4h** crystal packings contain voids most likely filled with disordered solvent. These voids formed very different channels from those proposed for Alm in the lipid membrane. In the **4g** and **4h** crystals, the helix and channel axes were perpendicular, while for Alm, they were expected to be parallel within the membrane (Figure S2-2).

View Article Online
DOI: 10.1039/C8OB00686E

Organic and Biomolecular Chemistry

ARTICLE

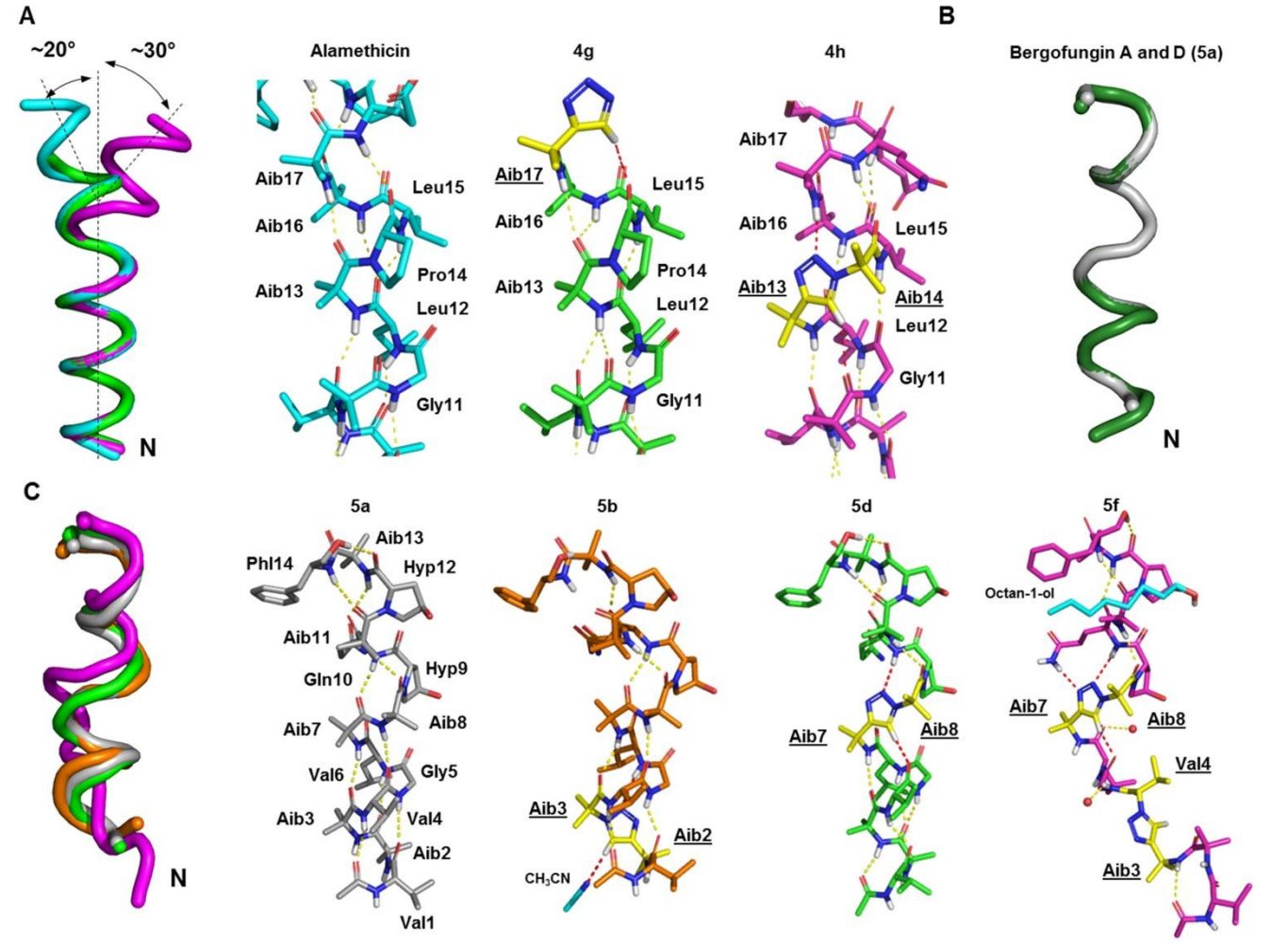

Figure 3. Crystal structures of the alamethicin, bergofungin D and their analogues with Tz insertions. A. Portion of the crystal structures of alamethicin (in cyan, PDB entry 1amt) and its analogues **4g** (in green) and **4h** (in magenta). Superimposition of their backbones in cartoon representation highlights the differences in C-terminal parts (bent orientations and bent amplitudes). B. Superimposition of the backbone in cartoon representation of the bergofungin A (in forest, PDB entry 5mas) and D (**5a**, in grey). C. Superimposition of the backbones in cartoon representation of the bergofungin D (**5a**, in grey) and analogs **5b** (in orange), **5d** (in green) and **5f** (in magenta). Hydrogen bond networks are shown as yellow dotted sticks while the hydrogen bonds involving the Tz rings are shown as red dotted sticks. Hydrogen atoms were omitted for clarity, except the amide protons and hydrogen atoms engaged in hydrogen bonds

We also solved the crystal structure of the BergD **5a**, which exhibited a kinked 3_{10} helix similar to those of the BergA recently reported,[34] and other natural analogues (Figure S2-3).[50] BergD is one residue shorter than BergA and the residue preceding the second hydroxyproline is an Aib residue instead of an isovaline (Figure S2-3). The 14 BergD residues fit well with the last 14 residues of BergA with an rmsd of 0.22 Å on Cα atoms (Figure 3B). Worth noting is that analogues **5b** and **5d** with Tz insertions in position 2-3 and 7-8 respectively, adopted similar conformations to BergD with rmsd of 0.84 Å and 0.63 Å on Cα atoms (Figures 3C and S2-4). We only noticed a small deviation of the **5b** N-terminus. When the first four residues were omitted, the rmsd decreased to 0.59 Å (Figure S2-4). Remarkably, in both structures, the Tz mimicked the amide bond that formed near complete hydrogen bond networks all along the helices (Figure 3C, Table S2-5). The N^2 atom of the Tz was engaged in a hydrogen bond with the NH amide of Leu^6 and Gln^{10} for **5b** and **5d**, respectively (d_{NH-N2} = 2.37 and 2.31 Å, respectively). The Tz-C^5-H of compound **5d** participated in a weak hydrogen bond with the carbonyl oxygen of Val^4 (d_{C5H-O} = 2.12 Å). In **5b**, the Tz-C^5-H at the N-terminal extremity could not be engaged in any intramolecular hydrogen bond but it formed a hydrogen bond with an acetonitrile molecule.

Importantly, we also succeeded in solving the structure of compound **5f** which contained a double Tz insertion in

View Article Online
DOI: 10.1039/C8OB00686F

positions 3-4 and 7-8. In contrast to compounds **5b** and **5d** with a single Tz insertion, only the last seven residues retained a helical conformation. The N-terminal moiety was rather extended containing a type 2 β-turn involving the two first residues (ϕ1 = -81°, ψ1 = 141°, ϕ2 = 60° and ψ2 = 27° (Figure 3C). Thus in a double insertion system, the peptide bond substitution between Aib[3] and Val[4] unwound the N-terminal part of the BergD helix, while the central Tz insertion between Aib[7] and Aib[8] was well tolerated. Interestingly, we observed in compound **5f** that the Tz-N[3] atom was also engaged in a backbone side chain hydrogen bond with the NHε of Gln[10] (d_{NH-N3} = 2.16 Å). As expected, while the CD spectroscopy allowed us to quickly determine the helix propensity for all compounds in solution, we noticed discrepancies with the solid-state structures. The Alm analogues **4a**, **4g** and **4h** shared similar helicities whereas the C-terminal moiety was disordered in the crystal for **4g**. In addition, despite fully helical folds for compounds **5b** and **5d** in solid-state, we observed that both Tz insertions strongly affected the 3_{10} helix signature of BergD. In this context, we further investigated the behavior of the analogues in solution via extensive NMR studies.

The NMR signals were well dispersed and assignment of ^{1}H, ^{13}C and ^{15}N chemical shifts were carried out combining homonuclear COSY, TOCSY, ROESY and heteronuclear ^{13}C-, ^{15}N-HSQC and ^{13}C-HMBC experiments (Tables S4). The Alm ^{3}J(HNHα) coupling constants were in the 4-6 Hz range from Ala[4] to Val[9] (Table S6-1). These values were characteristic of helical conformation and were similar to those reported by Esposito et al.[51] We first monitored the chemical shift variations of ^{1}HN, ^{15}N, ^{1}Hα, ^{13}Cα, and ^{13}CO backbone atoms upon the Tz insertions in the various analogues (Tables S5) and compared their $^{3}J(HNH_{\alpha})$ coupling constants (Table S6-1). While the backbone chemical shifts are widely used to identify the type and location of the secondary structures in proteins, we used them, here, to assess to what extent the Tz insertions alter the Alm and BergD helices. We noticed that the backbone atoms resonances were primarily altered around Tz rings for all analogues. Atoms in close vicinity were those with the highest variations solely due to the proximity of the Tz.

In general, the $^{3}J(HNH_{\alpha})$ values were very close to those of the native peptide even if slight variations occurred near the Tz insertion. Thus, single insertions may not impact the overall structure of Alm and BergD. In contrast, atomic resonances varied significantly along the entire backbone for cases with multiple Tz incorporations such as for **4i** and **4j**, but we could not discriminate whether they arose from current effects of Tz rings or from large structural alterations of these analogues. Nevertheless, few NOEs were observed on the ROESY spectra for both compounds and NMR structure calculations did not converge indicating that they were most likely not folded. Thus, we then focused on the other analogues and investigated the backbone geometry around the Tz using seven diagnostic NOE correlations identified from the crystal structure of the Tz-containing GCN4-pLI α-helical coiled coils (pdb ID 1U9F, Figure 4).[27] The presence of unambiguous NOE correlations between the $H_{\psi Tz}$(i) proton and the H_N(i-1), H_N(i+1), H_N(i-2), Hα(i-2), Hα(i-3), Hα(i-4) protons and Hα(i-3)-Hβ(i) were characteristic of local Tz-containing helix turns (Figure 3A). Solution NMR structures were then calculated using complete NOE sets as distance restraints. Although the $H_{\psi Tz}$(i)-H_N(i-2) and Hα(i-3)-Hβ(i) correlations were only detected in the ROESY spectra for a few compounds, the other probes were generally observed in the ROESY spectra for all analogues, except **5f**.

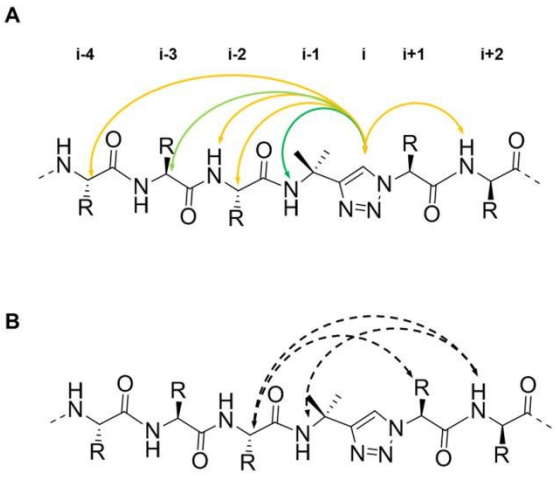

C

Compound	Position of the Tz (i, i+1)	Characteristic NOE cross-peaks and intensities						
		$H_{\psi Tz}$(i)-H_N(i-1)	$H_{\psi Tz}$(i)-H_N(i+1)	$H_{\psi Tz}$(i)- H_N(i-2)	$H_{\psi Tz}$(i)- Hα(i-2)	$H_{\psi Tz}$(i)-Hα(i-3)	$H_{\psi Tz}$(i)-Hα(i-4)	Hα(i-3)-Hβ(i)
4b	3-4	Weak	Weak	Nd	Weak	-	Weak	-
4c	5-6	Weak	Weak	Nd	Weak	-	Weak	-
4d	8-9	Weak	Weak	Nd	Weak	Weak	-	Nd
4e	10-11	Weak	Weak	Weak	Weak	-	Weak	Weak
4f	16-17	Weak	a	Nd	Weak	Weak	-	Weak
4g	17-18	Weak	Weak	Nd	-	Weak	Weak	Weak
4h	13-14	Weak	Weak	Nd	-	Weak	Weak	Nd
5b	2-3	Weak	a	Weak	Weak	Weak	-	-
5c	3-4	Weak	Nd	Nd	-	Weak	Weak	Nd
5d	7-8	Weak	-	a	a	Weak	Weak	-
5e	2-3	Weak	Weak	a	Weak	Weak	-	-
	7-8	Weak	-	Weak	Weak	Weak	Weak	-
5f	3-4	Weak	a	Nd	-	a	Nd	Nd
	7-8	a	-	Nd	Weak	Weak	Nd	-

Figure 4. A. Expected backbone NOE correlations surrounding the 1,2,3-triazole in Tz-containing helical template based on the crystal structure of GCN4-pLI coiled coils (pdb ID 1U9F). Strong, medium and weak NOEs are represented by green, light green and orange arrows, respectively. B. NOEs observed in the canonical α-helix but not expected in the analogues around the triazoles. C. Survey on the helix-consistent NOE correlations in the ROESY spectra of the analogues. *a*: ambiguous due to strong overlaps; *nd:* not detected

View Article Online
DOI: 10.1039/C8OB00686E

Organic and Biomolecular Chemistry

ARTICLE

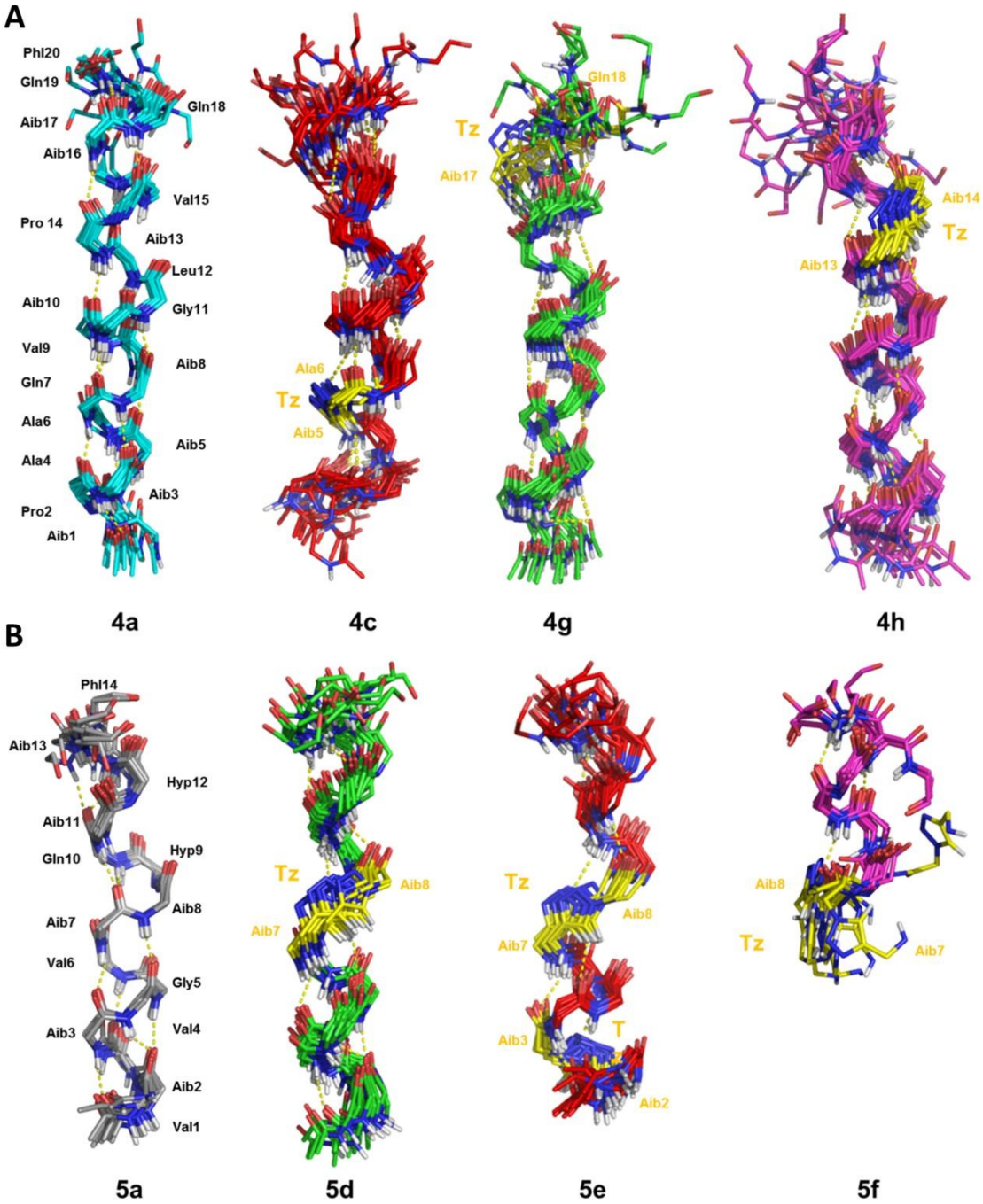

Figure 5: NMR structures of compounds A. **4a**, **4c**, **4g** and **4h** ; B. **5a**, **5d**, **5e** and **5f**

These results were in agreement with the set of crystal structures described above which were mostly helical while the N-terminal moiety of **5f** was extended. We calculated the NMR solution structures of **4c**, **4g**, **4h**, **5d**, **5e** and **5f** (Figure 5). As expected, whole analogues displayed helix structures in solution while the N-terminal extremity of **5f** was disordered. Through the use of NMR, we showed that the single Tz insertions within **4b-h** and **5b-d** did not alter the overall native

View Article Online
DOI: 10.1039/C8OB00685E

helical fold. However, the variations in CD signal intensities around 208 and 222 nm upon the incorporation of Tz in the Alm analogues reflected a loss of stability within the helices at varying degrees depending on the Tz position. The Alm helix was more prone to destabilization when the Tz were inserted in the center of the main 1-14 helix region, i.e, in positions 5-6 and 8-9 (Table 1, Figure S1). We also noticed that the variations of the BergD CD signature in response to Tz insertions (Figure 2) were not related to a complete loss of structure, for example **5b** and **5d** displayed helix crystal structures despite non-characteristic canonical CD profile. While the single Tz insertions in **5b** (2-3), and **5d** (7-8) did not affect their overall folds, the double insertions 2-3, 7-8 in **5e** and 3-4, 7-8 in **5f** led to various results. In the first case, the double insertion did not impact the helical structure, while in the latter the helix was partially unwound. Such results could be explained by the fact that **5c** should be less stable than **5b**. According to the general trend observed for the Alm analogues, the 2-3 substitution was less invasive than the 3-4. Therefore, **5e** could accommodate both the 2-3 and 7-8 substitutions while **5d** was only folded around the Tz rings in position 7-8.

Conclusions

Finally, in addition to the number and the position of Tz insertions in the peptide sequences, its nature and more specifically the types of amino acids surrounding the Tz ring should also be considered. Since the amino acids displayed various propensities for helix, coil and β-strand structures, one can anticipate that Tz dipeptide insertions should also affect the secondary structures of peptides and proteins. From our data, we first noticed that we obtained fully helical crystal structures for compounds **4h**, **5b** and **5d** which incorporated the Aib$_{[Tz]}$Aib dipeptides. Moreover, we observed in **5f** that the region containing the Aib$_{[Tz]}$Aib dipeptide was helical while the N-terminal moiety containing the Aib$_{[Tz]}$Val dipeptide was extended in solid-state and disordered in solution. We could reasonably conclude that the insertion of Tz between highly helicogen amino acids should be compatible. Nevertheless, the Alm analogues **4b** and **4c** incorporating the Aib$_{[Tz]}$Ala dipeptides in position 3-4 and 5-6 respectively, exhibited different results in solution. Although they displayed a similar NMR helix structure, the CD signal intensity value of **4c** at 220 nm dramatically increased to 2957 deg.cm^2.dmol^{-1} while it only increased to 8558 deg.cm^2.dmol^{-1} for **4b**. It is worth noting that a slightly shifted Aib$_{[Tz]}$Ala position yielded a vastly different stability outcome, **4c** being much less stable than **4b**. The relationship between the nature of the Xaa residue within Aib$_{[Tz]}$Xaa dipeptides and the helix stability was difficult to define.

In this study we revealed that the position of the Tz insertion resulted in a range of diverse structural features, from subtle rearrangements to large misfolding of the studied peptides. Single Tz insertions in the center of helices were more destabilizing than those on the extremities of the peptide sequences. The specific geometry of the Tz did not strictly substitute the amide bond and more importantly abolished the antimicrobial activity of Alm even when very slight conformational variations occurred. In this context, one should cautiously use the Tz as a *trans* peptide bond surrogate in helical peptides, especially when they exhibit close structure-activity relationships. Even if the overall peptide structure is conserved at the point of the Tz insertion, its stability and dynamics may be greatly impaired, resulting in the cessation of its biological activity.

Conflicts of interest

"There are no conflicts to declare".

Acknowledgements

We thank: Comité des Pyrénées Orientales de la Ligue Nationale Contre le Cancer and the Bonus Qualité Recherche of Perpignan University, MESR for financial support. The spectroscopic experiments have been performed at the "Laboratoire de mesures physiques" (LMP) at the University of Montpellier and using the Biodiversité et Biotechnologies Marines facilities (Bio2Mar, http://bio2mar.obs-banyuls.fr/fr/index.html) at the University of Perpignan, and the 'Plateforme de mesures de diffractionX' of the Université de Lorraine is appreciated. We are grateful to the staff members of the BM30A beamline at ESRF (Grenoble, France) and to our American colleague J Almany for comments and carefully proofreading of the manuscript.

Notes and references

1 H. C. Kolb, M. G. Finn and K. B. Sharpless, *Angew. Chem. Int. Ed.*, 2001, **40**, 2004–2021.
2 C. W. Tornøe, C. Christensen and M. Meldal, *J. Org. Chem.*, 2002, **67**, 3057–3064.
3 V. V. Rostovtsev, L. G. Green, V. V. Fokin and K. B. Sharpless, *Angew. Chem.*, 2002, **114**, 2708–2711.
4 Y. L. Angell and K. Burgess, *Chem. Soc. Rev.*, 2007, **36**, 1674–1689.
5 D. S. Pedersen and A. Abell, *Eur. J. Org. Chem.*, 2011, **2011**, 2399–2411.
6 X. Li, *Chem.- Asian J.*, 2011, **6**, 2606–2616.
7 J. M. Holub and K. Kirshenbaum, *Chem. Soc. Rev.*, 2010, **39**, 1325–1337.
8 V. D. Bock, D. Speijer, H. Hiemstra and J. H. van Maarseveen, *Org. Biomol. Chem.*, 2007, **5**, 971–975.
9 I. E. Valverde, F. Lecaille, G. Lalmanach, V. Aucagne and A. F. Delmas, *Angew. Chem.-Int. Ed.*, 2012, **51**, 718–722.
10 V. Aucagne, I. E. Valverde, P. Marceau, M. Galibert, N. Dendane and A. F. Delmas, *Angew. Chem. Int. Ed.*, 2012, **51**, 11320–11324.
11 A. D. Pehere, M. Pietsch, M. Gütschow, P. M. Neilsen, D. S. Pedersen, S. Nguyen, O. Zvarec, M. J. Sykes, D. F. Callen and A. D. Abell, *Chem. - Eur. J.*, 2013, **19**, 7975–7981.

12 S. Cantel, A. L. C. Isaad, M. Scrima, J. J. Levy, R. D. DiMarchi, P. Rovero, J. A. Halperin, A. M. D'Ursi, A. M. Papini and M. Chorev, *J. Org. Chem.*, 2008, **73**, 5663–5674.
13 M. Scrima, A. Le Chevalier-Isaad, P. Rovero, A. M. Papini, M. Chorev and A. M. D'Ursi, *Eur. J. Org. Chem.*, 2010, 446–457.
14 L. Frankiewicz, C. Betti, K. Guillemyn, D. Tourwé, Y. Jacquot and S. Ballet, *J. Pept. Sci.*, 2013, **19**, 423–432.
15 G. A. Patani and E. J. LaVoie, *Chem. Rev.*, 1996, **96**, 3147–3176.
16 M. Nahrwold, T. Bogner, S. Eissler, S. Verma and N. Sewald, *Org. Lett.*, 2010, **12**, 1064–1067.
17 E. Ko, J. Liu, L. M. Perez, G. Lu, A. Schaefer and K. Burgess, *J. Am. Chem. Soc.*, 2011, **133**, 462–477.
18 Y. Liu, L. Zhang, J. Wan, Y. Li, Y. Xu and Y. Pan, *Tetrahedron*, 2008, **64**, 10728–10734.
19 J. M. Beierle, W. S. Horne, J. H. van Maarseveen, B. Waser, J. C. Reubi and M. R. Ghadiri, *Angew. Chem.-Int. Ed.*, 2009, **48**, 4725–4729.
20 M. Tischler, D. Nasu, M. Empting, S. Schmelz, D. W. Heinz, P. Rottmann, H. Kolmar, G. Buntkowsky, D. Tietze and O. Avrutina, *Angew. Chem. Int. Ed.*, 2012, **51**, 3708–3712.
21 I. E. Valverde, A. Bauman, C. A. Kluba, S. Vomstein, M. A. Walter and T. L. Mindt, *Angew. Chem. Int. Ed.*, 2013, **52**, 8957–8960.
22 I. E. Valverde, S. Vomstein, C. A. Fischer, A. Mascarin and T. L. Mindt, *J. Med. Chem.*, 2015, **58**, 7475–7484.
23 M. Beltramo, V. Robert, M. Galibert, J.-B. Madinier, P. Marceau, H. Dardente, C. Decourt, N. De Roux, D. Lomet, A. F. Delmas, A. Caraty and V. Aucagne, *J. Med. Chem.*, 2015, **58**, 3459–3470.
24 A. Proteau-Gagné, K. Rochon, M. Roy, P.-J. Albert, B. Guérin, L. Gendron and Y. L. Dory, *Bioorg. Med. Chem. Lett.*, 2013, **23**, 5267–5269.
25 E. Gutiérrez-Pascual, J. Leprince, A. J. Martínez-Fuentes, I. Ségalas-Milazzo, R. Pineda, J. Roa, M. Duran-Prado, L. Guilhaudis, E. Desperrois, A. Lebreton, L. Pinilla, M.-C. Tonon, M. M. Malagón, H. Vaudry, M. Tena-Sempere and J. P. Castaño, *Mol. Pharmacol.*, 2009, **76**, 58–67.
26 B. P. Roques, C. Garbay-Jaureguiberry, R. Oberlin, M. Anteunis and A. K. Lala, *Nature*, 1976, **262**, 778–779.
27 W. S. Horne, M. K. Yadav, C. D. Stout and M. R. Ghadiri, *J. Am. Chem. Soc.*, 2004, **126**, 15366–15367.
28 T. Boddaert, J. Solà, M. Helliwell and J. Clayden, *Chem. Commun.*, 2012, **48**, 3397.
29 N. Kann, J. R. Johansson and T. Beke-Somfai, *Org. Biomol. Chem.*, 2015, **13**, 2776–2785.
30 R. O. Fox Jr and F. M. Richards, *Nature*, 1982, **300**, 325–330.
31 A. Berg, M. Ritzau, W. Ihn, B. Schlegel, W. F. Fleck, S. Heinze and U. Grafe, *J. Antibiot. (Tokyo)*, 1996, **49**, 817–820.
32 S. Aravinda, N. Shamala, R. S. Roy and P. Balaram, *J. Chem. Sci.*, 2003, **115**, 373–400.
33 G. R. Marshall, E. E. Hodgkin, D. A. Langs, G. D. Smith, J. Zabrocki and M. T. Leplawy, *Proc. Natl. Acad. Sci.*, 1990, **87**, 487–491.
34 R. Gessmann, D. Axford, H. Brückner, A. Berg and K. Petratos, *Acta Crystallogr. Sect. F Struct. Biol. Commun.*
35 L. Kredics, A. Szekeres, D. Czifra, C. Vágvölgyi and B. Leitgeb, *Chem. Biodivers.*, 2013, **10**, 744–771.
36 T. Nagao, D. Mishima, N. Javkhlantugs, J. Wang, D. Ishioka, K. Yokota, K. Norisada, I. Kawamura, K. Ueda and A. Naito, *Biochim. Biophys. Acta BBA - Biomembr.*, 2015, **1848**, 2789–2798.
37 K. Ben Haj Salah, B. Legrand, S. Das, J. Martinez and N. Inguimbert, *Pept. Sci.*, 2015, **104**, 611–621.
38 S. Das, K. Ben Haj Salah, E. Wenger, J. Martinez, J. Kotarba, V. Andreu, N. Ruiz, F. Savini, L. Stella, C. Didierjean, B. Legrand and N. Inguimbert, *Chem. – Eur. J.*, 2017, **23**, 17964–17972.
39 K. Ben Haj Salah and N. Inguimbert, *Org. Lett.*, 2014, **16**, 1783–1785.
40 R. Fanelli, K. B. H. Salah, N. Inguimbert, C. Didierjean, J. Martinez and F. Cavelier, *Org. Lett.*, 2015, **17**, 4498–4501.
41 G. Jung, W. A. König, D. Leibfritz, T. Ooka, K. Janko and G. Boheim, *Biochim. Biophys. Acta BBA - Biomembr.*, 1976, **433**, 164–181.
42 G. Yoder, A. Polese, R. A. G. D. Silva, F. Formaggio, M. Crisma, Q. B. Broxterman, J. Kamphuis, C. Toniolo and T. A. Keiderling, *J. Am. Chem. Soc.*, 1997, **119**, 10278–10285.
43 N. H. Andersen, Z. Liu and K. S. Prickett, *FEBS Lett.*, 1996, **399**, 47–52.
44 M. Bellanda, S. Mammi, S. Geremia, N. Demitri, L. Randaccio, Q. B. Broxterman, B. Kaptein, P. Pengo, L. Pasquato and P. Scrimin, *Chem. – Eur. J.*, 2007, **13**, 407–416.
45 J. Jacob, H. Duclohier and D. S. Cafiso, *Biophys. J.*, 1999, **76**, 1367–1376.
46 Y. Nagaoka, A. Iida, E. Tachikawa and T. Fujita, *Chem. Pharm. Bull. (Tokyo)*, 1995, **43**, 1119–1124.
47 H. Vogel, *Biochemistry (Mosc.)*, 1987, **26**, 4562–4572.
48 H.-H. Nguyen, D. Imhof, M. Kronen, U. Gräfe and S. Reissmann, *J. Pept. Sci.*, 2003, **9**, 714–728.
49 J. Taira, M. Shibue, S. Osada and H. Kodama, *Int. J. Pept. Res. Ther.*, 2010, **16**, 277–282.
50 M. De Zotti, B. Biondi, C. Peggion, Y. Park, K.-S. Hahm, F. Formaggio and C. Toniolo, *J. Pept. Sci.*, 2011, **17**, 585–594.
51 G. Esposito, J. A. Carver, J. Boyd and I. D. Campbell, *Biochemistry (Mosc.)*, 1987, **26**, 1043–1050.

View Article Online
DOI: 10.1039/C8OB00686E

Peptaibols were used as templates to monitor the impact of 1,2,3-triazole (Tz) insertion in place of amide bonds in helix structures.

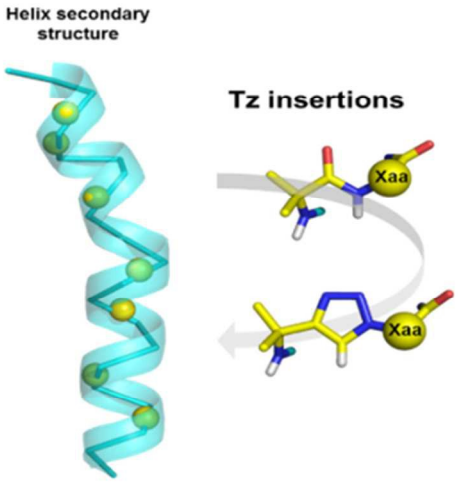

79x39mm (300 x 300 DPI)